Rat subicular networks gate hippocampal output activity in an *in vitro* model of limbic seizures

Ruba Benini[1] and Massimo Avoli[1,2]

[1] *Montreal Neurological Institute and Departments of Neurology & Neurosurgery, and of Physiology, McGill University, Montreal, QC, H3A 2B4, Canada*
[2] *Dipartimento di Fisiologia Umana e Farmacologia, Università di Roma 'La Sapienza', 00185 Rome, Italy*

Evidence obtained from human epileptic tissue maintained *in vitro* indicates that the subiculum may play a crucial role in initiating epileptiform discharges in patients with mesial temporal lobe epilepsy. Hence, we used rat hippocampus–entorhinal cortex (EC) slices to identify the role of subiculum in epileptiform synchronization during bath application of 4-aminopyridine (4AP, 50 μM). In these slices, fast CA3-driven interictal-like events were restricted to the hippocampal CA3/CA1 areas and failed to propagate to the EC where slow interictal-like and ictal-like epileptiform discharges were recorded. However, antagonizing $GABA_A$ receptors with picrotoxin (50 μM) made CA3-driven interictal activity spread to EC. Sequential field potential analysis along the CA3–CA1–subiculum axis revealed that the amplitude of CA3-driven interictal discharges recorded in the presence of 4AP only diminished within the subiculum. Furthermore, CA1 electrical stimulation under control conditions elicited little or no subicular activation and never any response in EC; in contrast, robust subicular discharges that spread to EC could be evoked after picrotoxin. Intracellular recordings indicated that potentiation by picrotoxin was associated with blockade of hyperpolarizing IPSPs in subicular cells. Finally, when surgically isolated from adjacent structures, the subiculum generated low-amplitude synchronous discharges that corresponded to an intracellular hyperpolarization–depolarization sequence, were resistant to glutamatergic antagonists, and represented the activity of synchronized interneuronal networks. Bath application of picrotoxin abolished these 4AP-induced events and in their place robust network bursting occurred. In conclusion, our study demonstrates that the subiculum plays a powerful gating role on hippocampal output activity. This function depends on $GABA_A$ receptor-mediated inhibition and controls hippocampal–parahippocampal interactions that are known to modulate limbic seizures.

(Resubmitted 15 April 2005; accepted after revision 31 May 2005; first published online 2 June 2005)
Corresponding author M. Avoli: 3801 University, room 794, Montreal, QC, Canada H3A 2B4.
Email: massimo.avoli@mcgill.ca

Mesial temporal lobe epilepsy (MTLE) is one of the most common types of partial epilepsy in humans (Wiebe, 2000). MRI images from MTLE patients are often characterized by hippocampal atrophy which, upon histological examination, reveals extensive neuronal loss and gliosis in the dentate hilus and CA3/CA1 areas along with synaptic reorganization (Sutula *et al.* 1989; Houser *et al.* 1990). In addition, neuronal damage in this epileptic disorder is seen in limbic areas such as the entorhinal cortex (EC) and the amygdala (Du *et al.* 1993; Gloor, 1997; Pitkanen *et al.* 1998; Houser, 1999; Yilmazer-Hanke *et al.* 2000). Histopathological analysis of human epileptic tissue has also shown that subicular principal cells are relatively unaffected in MTLE (Gloor, 1997). Nevertheless, the absence of neuronal loss in the subiculum does not exclude the possibility that this area may play an active role in MTLE. Indeed, recent studies in both human (Cohen *et al.* 2002; Wozny *et al.* 2003) and animal (Behr & Heineman, 1996; D'Antuono *et al.* 2002; Wellmer *et al.* 2002) epileptic tissue suggest that cellular and synaptic reorganization in the subiculum contributes to limbic seizure generation.

The subiculum holds a strategic position within the limbic system. Not only does it serve as the major output structure of the hippocampus, getting extensive projections from the CA1 hippocampal region (Finch & Babb, 1981; Witter *et al.* 1989), but it also projects to various limbic and extralimbic areas including EC layers IV and V (Swanson & Cowan, 1977; Witter *et al.* 1989), perirhinal cortex (Swanson *et al.* 1978; Deacon *et al.* 1983), amygdala (Canteras & Swanson, 1992) and thalamus (Witter *et al.* 1990; Canteras & Swanson, 1992)

 DOI: 10.1113/jphysiol.2005.088708

(see for review O'Mara *et al.* 2001). In this study, we sought to identify the role played by the subiculum in intralimbic synchronization using the 4-aminopyridine (4AP) *in vitro* model of limbic seizures. Here, we report that $GABA_A$ receptor-mediated mechanisms confer on the subiculum the ability to gate hippocampal output activity, and thus to dictate the interactions between hippocampal and parahippocampal neuronal networks.

Methods

Male, adult Sprague-Dawley rats (150–200 g) were decapitated under halothane anaesthesia according to the procedures established by the Canadian Council of Animal Care. The brain was quickly removed and a block of brain tissue containing the retrohippocampal region was placed in cold (1–3°C), oxygenated artificial cerebrospinal fluid (ACSF). The brain's dorsal side was cut along a horizontal plane that was tilted by a 10 deg angle along a postero-superior-anteroinferior plane passing between the lateral olfactory tract and the base of the brainstem (Avoli *et al.* 1996). Horizontal slices (450–500 μm) containing the EC and the hippocampus were cut from this brain block using a vibratome. Subicular minislices were prepared from these horizontal slices by using microknife cuts to isolate the subiculum from the other hippocampal and parahippocampal structures (Fig. 7*B*). Slices were then transferred into a tissue chamber where they lay at the interface between ACSF and humidified gas (95% O_2, 5% CO_2) at a temperature of 34–35°C and a pH of 7.4. ACSF composition was (mM): NaCl 124, KCl 2, KH_2PO_4 1.25, $MgSO_4$ 2, $CaCl_2$ 2, $NaHCO_3$ 26, and glucose 10. 4AP (50 μM), bicuculline methobromide (BMI, 10 μM), 6-cyano-7-nitroquinoxaline-2,3-dione (CNQX, 10 μM), 3,3-(2-carboxypiperazin-4-yl)-propyl-1-phosphonate (CPP, 10–30 μM), and picrotoxin (PTX, 50 μM) were applied to the bath. Chemicals were acquired from Sigma (St Louis, MO, USA) with the exception of BMI, CNQX and CPP, which were obtained from Tocris Cookson (Ellisville, MO, USA).

Field potential recordings were made with ACSF-filled, glass pipettes (resistance = 2–10 MΩ) that were connected to high-impedance amplifiers. The location of the recording electrodes in the combined hippocampus–EC slice is shown in Fig. 2*A*. Field responses were induced by applying single shock electrical stimuli (50–100 μs; < 200 μA) delivered through a bipolar, stainless steel electrode (Fig. 3*A*). Sharp-electrode intracellular recordings were performed in the subiculum with pipettes that were filled with 3 M potassium acetate (tip resistance = 70–120 MΩ). Intracellular signals were fed to a high-impedance amplifier with internal bridge circuit for intracellular current injection. The resistance compensation was monitored throughout the experiment and adjusted as required. The passive membrane properties of the subicular cells included in this study were measured as follows: (i) resting membrane potential (RMP) after cell withdrawal; (ii) apparent input resistance (R_i) from the maximum voltage change in response to a hyperpolarizing current pulse (100–200 ms, < -0.5 nA); (iii) action potential amplitude (APA) from the baseline; and (iv) action potential duration (APD) at half-amplitude. Intrinsic firing patterns of subicular cells were determined from responses to depolarizing current pulses of 500–1000 ms duration. Three neuronal types could be distinguished in this study: strong bursters, weak bursters and regular firing (Staff *et al.* 2000). Since no differences were observed between these classes in terms of their 4AP-induced activity, strong and weak intrinsic bursters were put together in the 'bursting' group (Fig. 5*Ab*) whilst regular firing cells were placed in the 'non-bursting' category (Fig. 6*Ab*). No fast spiking cells were ever recorded in this study.

Field potential and intracellular signals were fed to a computer interface (Digidata 1322A, Axon Instruments) and acquired and stored using the pCLAMP 9 software (Axon Instruments). Subsequent analysis of these data was made with the Clampfit 9 software (Axon Instruments). For time-delay measurements, the onset of the field potential/intracellular signals was established as the time of the earliest deflection of the baseline recording (e.g. inset traces in Fig. 1*A* and *B*). Throughout this study we arbitrarily termed as 'interictal' and 'ictal' the synchronous epileptiform events with durations shorter or longer than 2 s, respectively (cf. Traub *et al.* 1996). Measurements in the text are expressed as means ± S.D. and n indicates the number of slices or neurones studied under each specific protocol. Data were compared with Student's t test and were considered statistically significant if $P < 0.05$.

Results

Epileptiform activity induced by 4AP in combined hippocampus-EC slices

As illustrated in Fig. 1*A* (Control (4AP)) and Fig. 2*A*, the hippocampus–EC slices ($n = 110$) included in this study responded to 4AP application by generating three types of synchronous activities (cf. Avoli *et al.* 1996; Benini *et al.* 2003): (i) fast interictal discharges (interval of occurrence = 1.6 ± 0.7 s; duration 139 ± 65 ms; $n = 25$) that were restricted to the hippocampus proper (Fig. 1*A*, arrows); (ii) slow interictal events that were recorded in both hippocampal and EC regions and could initiate anywhere in the slice (interval of occurrence = 28 ± 15 s; $n = 25$; Fig. 1*A*, asterisk); and (iii) long-lasting ictal discharges (interval of occurrence = 236 ± 117 s; duration 64 ± 56 s; $n = 25$) that originated in EC and could propagate to the hippocampus via the perforant pathway

(Fig. 1*A*, bar). We termed these slices functionally disconnected due to the lack of epileptiform activity propagation from the hippocampus to the EC.

Involvement of $GABA_A$ receptors in the epileptiform activity induced by 4AP

Next, we superfused these slices with the $GABA_A$ receptor antagonist picrotoxin (50 μM) to establish the role of $GABA_A$ receptor-mediated mechanisms in 4AP-induced epileptiform discharges. As shown in Fig. 1, picrotoxin application to these functionally disconnected slices ($n = 45$) resulted in a dramatic change in the 4AP-induced electrographic activity (Figs 1 and 2). Exposure to this non-competitive $GABA_A$ receptor antagonist triggered an initial ictal burst in the EC (Fig. 2*B*, + Picrotoxin) after which the activity was replaced by robust interictal discharges that initiated in CA3 and propagated sequentially to CA1 and EC (expanded trace in the inset of Fig. 1*B*, + Picrotoxin). This phenomenon was reproduced with the competitive $GABA_A$ receptor antagonist BMI (10 μM, $n = 4$), thus suggesting that the effect observed was indeed due to hindrance of $GABA_A$ receptor function. Transformation of a functionally disconnected slice into one in which hippocampus-driven epileptiform activity could propagate to the EC was fully reversible upon washing out picrotoxin ($n = 6$) for approx. 2 h (not shown).

$GABA_A$ receptor antagonism potentiates interictal activity in the subiculum of functionally disconnected slices

To gain a better understanding of how $GABA_A$ receptor antagonism in functionally disconnected slices leads to synchronicity between hippocampus and EC, we analysed the 4AP-induced activity in neuronal networks along the CA3–CA1–subiculum axis ($n = 14$). This was achieved by obtaining simultaneous field potential recordings from CA3 and EC with two fixed electrodes while a third electrode was moved sequentially from the CA1–CA2 area towards the subiculum at the level of the stratum pyramidale. We found in six of these experiments that the CA3-driven interictal events had similar amplitudes up to the CA1–subiculum border (Fig. 2*Ab*, Control, +4AP) and then decreased as the recording electrode was placed in subiculum (Fig. 2*Ac*, Control, +4AP). Moreover, in the remaining experiments ($n = 8$) interictal events were not recorded during 4AP application in the subiculum concomitant with those seen in the CA3 and CA1 areas (Fig. 4*A*).

Following picrotoxin application (Fig. 2*B*, + Picro toxin), there was a potentiation in the amplitude of the epileptiform activity recorded within the subiculum. Moreover, such augmentation always occurred prior to the establishment of complete synchronization of the epileptiform activity between hippocampus and EC (Fig. 2*B*, + Picrotoxin, middle inset). Quantitative analysis of the picrotoxin-induced changes in field potential amplitudes in CA3, CA1 and subiculum revealed that the most drastic potentiation (314 ± 163%, $n = 6$) occurred

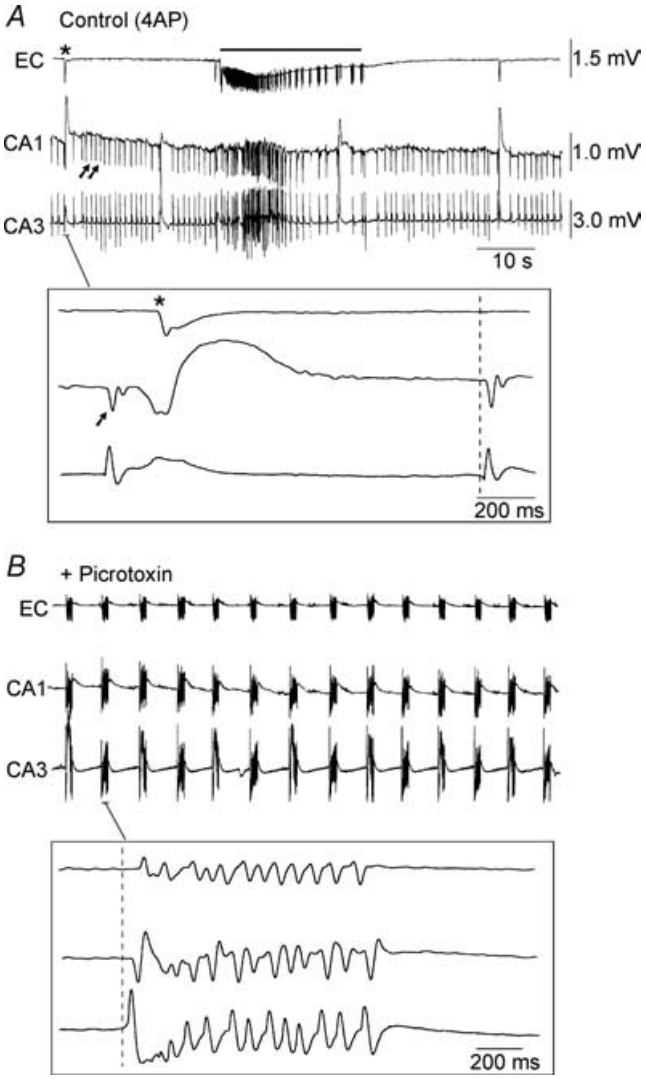

Figure 1. Effect of picrotoxin on 4AP-induced activity in a combined hippocampus–EC slice
A, simultaneous field potential recordings obtained from EC, CA1 and CA3 during bath application of 4AP. Note that fast interictal discharges (arrows in the CA1 trace) are restricted to the hippocampus (CA3 and CA1) but that slow interictal events (asterisk in the EC trace) are recorded in both hippocampus and EC. Note also the long-lasting ictal discharge (bar). *B*, picrotoxin application causes loss of ictal discharge in the EC and the appearance of robust interictal discharges that initiate in CA3 and propagate sequentially to CA1 and EC (inset). The insets in *A* and *B* show selected interictal events at faster time bases and the dashed lines demonstrate that these discharges initiate in CA3.

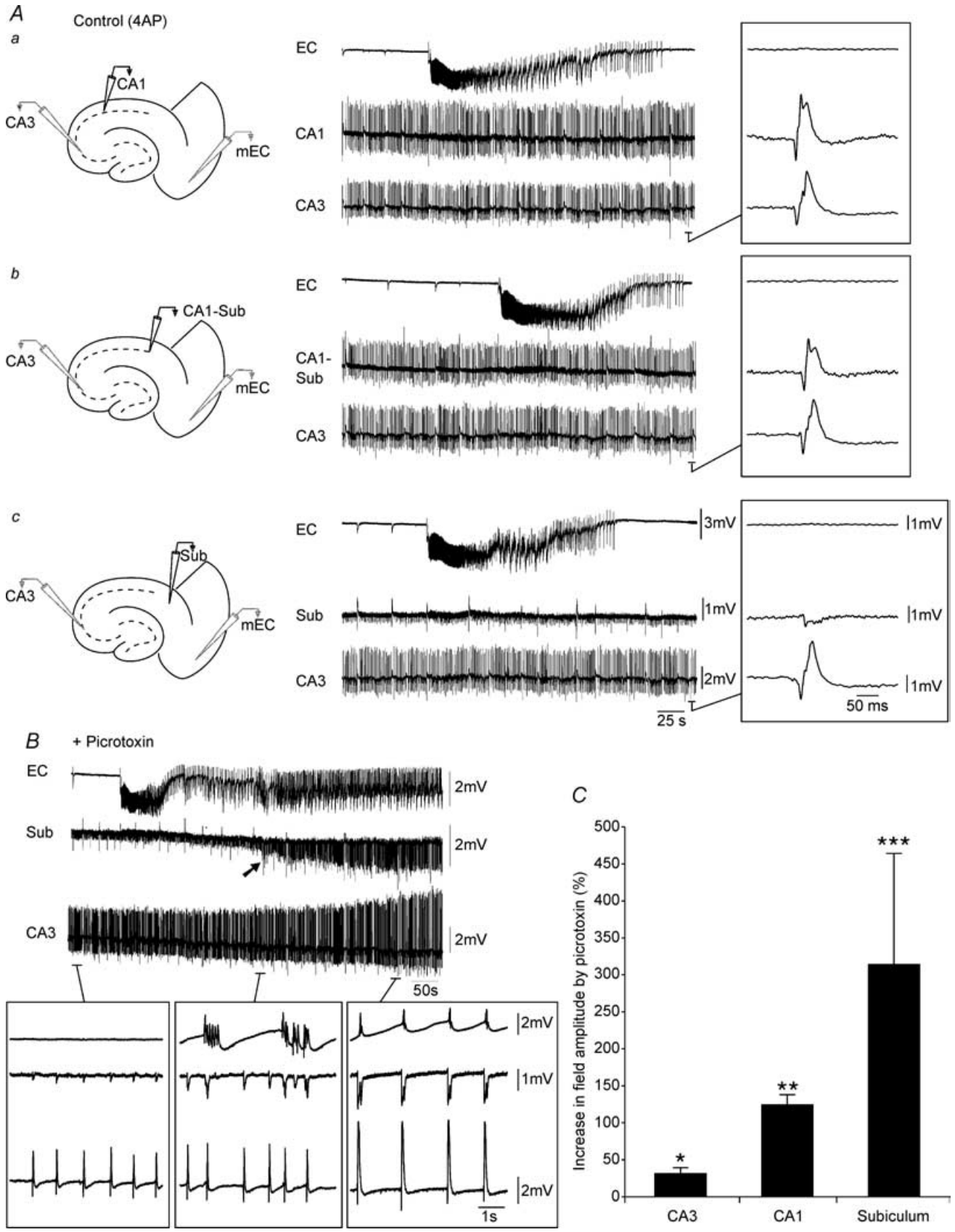

within the last structure whereas the least augmentation took place in CA3 ($31 \pm 8\%$; $n = 6$) (Fig. 2*C*).

Stimulation of hippocampal networks elicits response in EC only under $GABA_A$ receptor antagonism

To explore further the propagation of hippocampus-driven activity to the EC, we investigated the responses induced in the slice by focal electrical stimuli delivered in CA1, subiculum and EC: (i) in the absence of convulsants (i.e. normal ACSF); (ii) in the presence of 4AP; and (iii) during application of 4AP + PTX (Fig. 3*A*, *B* and *C*, respectively). In these experiments, three recording electrodes were placed in CA1 stratum pyramidale, subiculum and EC deep layers while a stimulating electrode was used to sequentially activate each of these structures.

As expected, a local field response could be recorded in any of the stimulated structures during application of normal ACSF (Fig. 3*Aa–c*, arrows); in addition, EC stimulation could also elicit some responses in subiculum and CA1. Following 4AP application (Fig. 3*B*), the local responses increased in amplitude and duration while distant activation could be clearly identified when stimuli were delivered in subiculum and EC (Fig. 3*Bb* and *c*, respectively); in contrast, as seen in normal medium, CA1 single shock stimuli (Fig. 3*Ba*) failed in eliciting subicular ($n = 12$) or EC responses ($n = 24$). Finally, during concomitant application of 4AP and picrotoxin, electrical stimuli delivered in any area of the slice induced robust epileptiform discharges in all limbic structures (Fig. 3*Ca–c* (4AP + PTX)). It should be emphasized that CA1 single-shock stimuli delivered during $GABA_A$-receptor antagonism (Fig. 3*Ca*) elicited an epileptiform response not only in subiculum, but also in EC ($n = 6$). Therefore, these observations suggest that $GABA_A$ receptor-mediated mechanisms prevent the propagation of both stimulation- and 4AP-induced hippocampal activity to the EC, thereby confirming that the functional disconnectivity between the hippocampus proper and EC was not merely an artifact of the 4AP model itself. In addition, both the potentiation of subicular responses by picrotoxin and the subsequent ability of hippocampus-driven discharges to propagate to the EC suggest that these inhibitory restrictions are most likely at play in the subiculum itself.

Picrotoxin-induced changes in connectivity do not require NMDA receptor function

We also assessed whether NMDA receptors contributed to the changes in connectivity seen during picrotoxin application. To this end we applied high concentrations of the NMDA-receptor antagonist CPP to functionally disconnected slices. As shown in Fig. 4*B* (+ 30 μM CPP, $n = 5$) CPP abolished the 4AP-induced ictal events that initiated in EC (Avoli *et al.* 1996; de Guzman *et al.* 2004). However, further addition of picrotoxin could still cause an initial ictal event followed by interictal activity in all areas of the slice (Fig. 4*C*, + 30 μM CPP + 50 μM Picrotoxin). Furthermore, NMDA receptor blockade did not avert the picrotoxin-induced potentiation of the interictal activity or its appearance in the subiculum. (Fig. 4*C*; $n = 5$).

Simultaneous field potential and intracellular recordings in the subiculum

The results obtained from the functionally disconnected slices during application of medium containing only 4AP suggest that the subiculum plays a role in gating hippocampal output activity. Furthermore, the ability of CA3-driven epileptiform discharges to propagate to the EC during picrotoxin suggests GABAergic mechanisms in the subiculum might be involved in such a control. Hence, we recorded intracellularly subicular cells along with field potential activity in CA3 and EC in the presence of 4AP and following further addition of picrotoxin.

Two main modes of subicular activity were recorded from these slices during 4AP application. The first type was seen in 20 subicular cells and consisted of bursts of action potentials that followed the interictal discharges recorded in CA3 with time lags of 21 ± 9 ms ($n = 7$) (Fig. 5). Electrophysiological characterization of these neurones revealed that 9 out of 20 cells were intrinsic non-bursters (RMP = -62.9 ± 7.2 mV, $R_i = 66.4 \pm 16.3$ MΩ, APA = 93.5 ± 13.3 mV, APD = 1.0 ± 0.2 ms; not shown) while the remaining 11

Figure 2. Picrotoxin-induced augmentation of field amplitudes in CA3, CA1 and subiculum
A, sequential field potential recording along the CA3–CA1–subiculim (Sub)–EC axis under control (4AP) conditions. Field electrodes in CA3 and EC were kept at the same position whilst a third electrode was moved along the stratum pyramidale to CA1 (*a*), CA1–Sub border (*b*) and Sub (*c*). Note the diminished field activity recorded in the subiculum as compared to CA1 and CA1–subiculum. *B*, monitoring field potential activity in EC, subiculum and CA3 from the onset of picrotoxin application until complete synchronization of the limbic structures. Note that initially CA3-driven interictal discharges do not propagate to the EC (left lower inset), but that following potentiation of subicular network activity (arrow), CA3-driven interictal events can propagate to the EC (right lower inset). Also note that potentiation in subicular activity precedes hippocampus–EC synchronization (middle *versus* right inset). *C*, bar graph of the normalized increase in field potential amplitude recorded in different areas of the slice; note that the most drastic potentiation occurs in the subiculum.

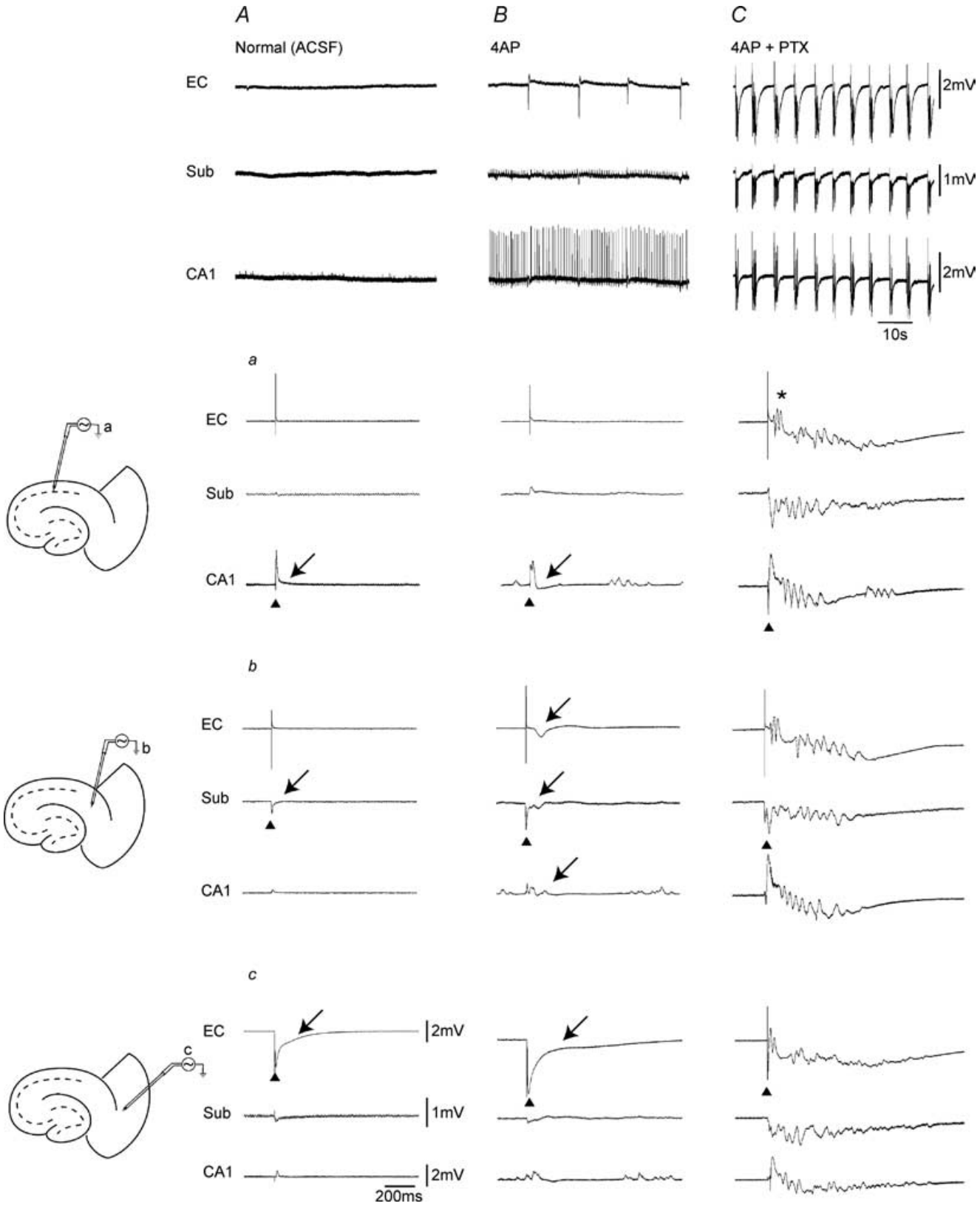

cells (RMP = −63.4 ± 7.0 mV, R_i = 60.9 ± 15.6 MΩ, APA = 94.5 ± 6.8 mV, APD = 1.0 ± 0.1 ms) discharged action potential bursts at the onset of an intracellular depolarizing pulse (Fig. 5*Ab*). Application of picrotoxin to these slices resulted in synchronous interictal discharges occurring in all areas. Furthermore, expanded traces demonstrated that these intracellular events followed CA3 field activity and preceded that of the EC (Fig. 5*B*, Picrotoxin (late), inset). Intracellular injection of depolarizing pulses indicated that picrotoxin did not modify the intrinsic firing patterns of these cells (not shown).

In contrast, the second group of subicular cells (n = 11) generated little or no spontaneous action potential firing, while producing robust postsynaptic potentials (PSPs) in association with the CA3-recorded interictal discharges (Fig. 6*Aa*, Control (4AP)). These PSPs were usually predominated by a hyperpolarizing component (Fig. 6*A*, Control (4AP), arrows in the lower inset) with a reversal value of approx. −71 mV (not illustrated) suggesting that they were $GABA_A$ receptor mediated. In addition, these neurones also generated large isolated hyperpolarizing potentials (Fig. 6*A*, Control (4AP), asterisk in the lower inset) with a similar reversal potential. Examination of the firing properties of these cells (Fig. 6*Ab*) revealed that 9 out of 11 were non-bursting elements (RMP = −67.7 ± 5.1 mV, R_i = 57.2 ± 14.3 MΩ, APA = 99.2 ± 5.4 mV, APD = 1.2 ± 0.1 ms). Superfusion of these slices with picrotoxin transformed the activity of these 'silent' cells into synchronous burst firing (Fig. 6*Aa*, Picrotoxin). Monitoring the evolution in the intracellular activity of these neurones from the onset of picrotoxin application (Fig. 6*Aa*, Picrotoxin (transition)) until the complete synchronization between hippocampal areas and EC (Fig. 6*Aa*, Picrotoxin, late) revealed a gradual decrease in the frequency of occurrence and the eventual disappearance of the robust PSPs (Fig. 6*Aa*, Picrotoxin (transition) *versus* Picrotoxin (late)) along with the complete blockade of the isolated hyperpolarizing potentials. As with the other group of subicular cells, the intrinsic firing patterns of these neurones were not changed by picrotoxin (not shown).

Picrotoxin-induced potentiation in subicular activity is not due to upstream effects

It has been well documented that GABAergic circuits exert an important inhibitory control over local networks within CA3/CA1; in addition, loss of this restraint via $GABA_A$ receptor antagonism is sufficient to unmask polysynaptic glutamatergic excitation within these structures (Miles & Wong, 1987; Miles *et al.* 1988). Hence, it can be reasonably argued that the picrotoxin-induced potentiation of subicular activity observed in our experiments might arise from enhanced, upstream hippocampal output rather than decreased gating within the subiculum. In order to clarify this issue, bath application of picrotoxin was investigated in slices in which the subiculum was isolated from CA3/CA1 by knife-cuts to the Schaffer collaterals (Fig. 7*Aa*). In this set of experiments, potentiation of subicular activity upon $GABA_A$ receptor antagonism was observed to occur in spite of the cut (n = 6, Fig. 7*Ab*, + Picrotoxin). However, epileptiform discharges in this scenario appeared to initiate sometimes in the subiculum (n = 3 slices) and at other times in the EC (n = 3 slices) (Fig. 7*Ab*, inset).

The potential gating role of subicular networks was further addressed in isolated subicular minislices (Fig. 7*B*). In the presence of 4AP, low-amplitude synchronous discharges (interval of occurrence = 142 ± 107 s; 55–450 s; n = 18) were observed to occur in all areas of the isolated subiculum and could initiate in the proximal, middle or distal regions (Fig. 7*Ba*, Control (4AP)). Subsequent addition of picrotoxin induced a drastic augmentation of activity in all subicular regions (n = 13, Fig. 7*Ba*, + Picrotoxin) thereby providing conclusive evidence that during 4AP application subicular networks, both in the combined slice and the isolated minislice preparations, are under tight $GABA_A$ receptor-mediated control.

Slow 4AP-induced interictal discharges generated in the subiculum represent the activity of synchronized interneuronal networks

Intracellular characterization of the slow-interictal discharges recorded in subicular minislices revealed a

Figure 3. Stimulation of hippocampal outputs activates EC only under conditions of $GABA_A$-receptor antagonism

Panels in the top row show the spontaneous field potential activity recorded simultaneously from CA1, subiculum and EC in the absence of convulsants (i.e. Normal ACSF) (*A*), in the presence of 4AP (*B*), and during 4AP + PTX (*C*). Slice diagrams on the left illustrate the positions of the stimulating bipolar electrode in CA1 (*a*), subiculum (*b*), and deep EC layer (*c*). Triangles indicate the structure stimulated in each set of recordings and arrows point to the subsequent response recorded. Note that single shock stimulation of CA1 networks both in the absence and presence of 4AP induces a small subicular response with no EC activation (*Aa* and *Ba*). Note in contrast the potentiated subicular response and the subsequent EC discharge (asterisk) induced by hippocampal output stimulation under $GABA_A$-receptor antagonism (*Ca*).

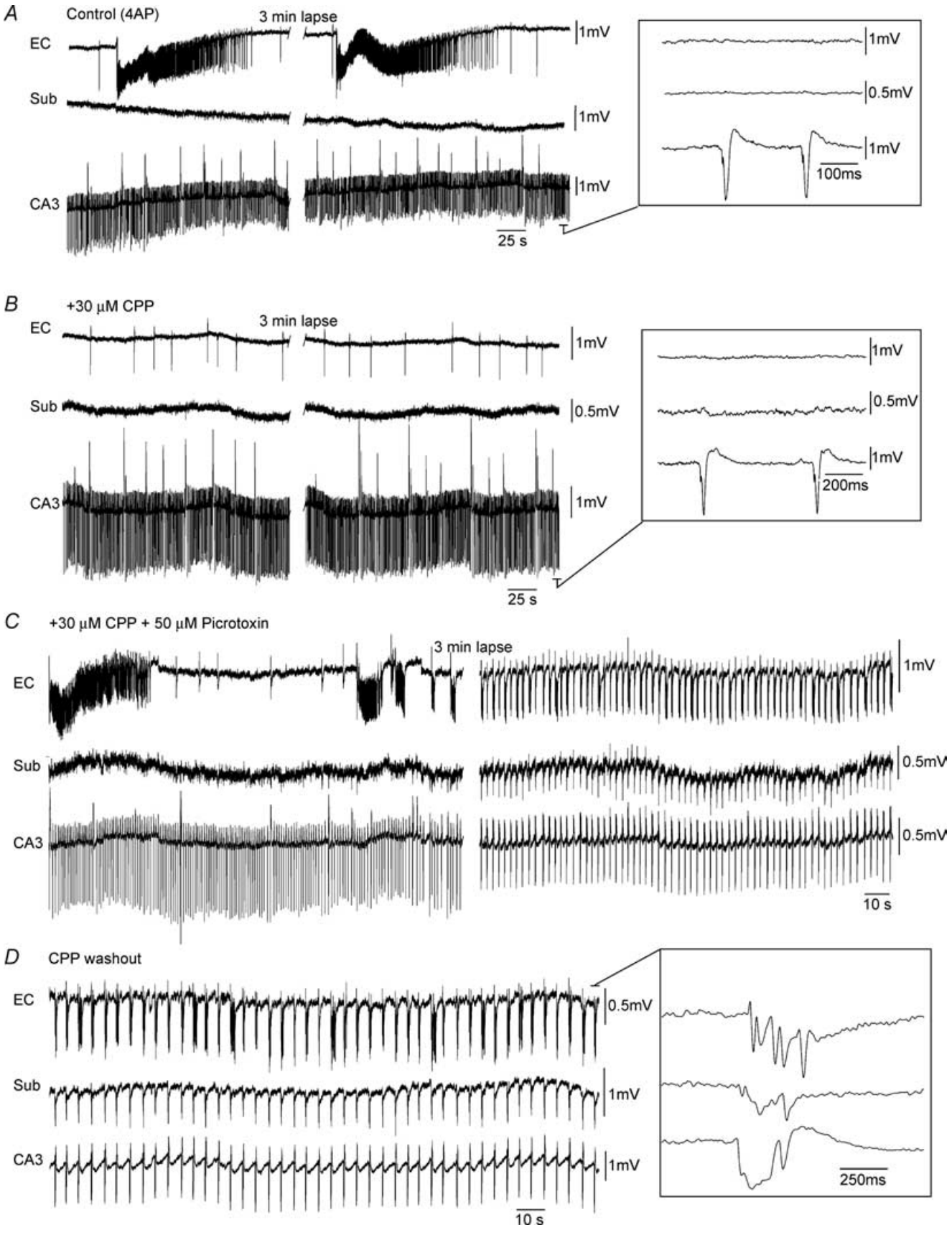

sequence of an early hyperpolarizing IPSP followed by a long lasting depolarization that could at times trigger action potential firing (Fig. 8*Aa* and *b* and *B*, Control (4AP); $n = 20$ neurones). Bath application of picrotoxin abolished these events and in their place robust network bursting was observed ($n = 6$ neurones, Fig. 8*Aa*, + Picrotoxin).

To further investigate the mechanisms underlying the generation of these 4AP-induced slow events, glutamatergic antagonists were employed. Interestingly, CPP and CNQX could not abolish these low amplitude discharges (Fig. 8*B*, + (CP P+ CNQX), $n = 8$) while further application of picrotoxin resulted in their complete loss ($n = 4$, not shown). Thus, these results indicate that as in other cortical areas (Perreault & Avoli, 1989, 1992; Avoli *et al.* 1994, 1996) the synchronous potentials recorded in the subiculum in the presence of 4AP correspond to the responses of pyramidal cells to the synchronized interneurone activity.

Discussion

We have found here that decreasing $GABA_A$ receptor function facilitates communication within the limbic networks contained in a combined hippocampus–EC slice. Accordingly, picrotoxin transformed functionally disconnected slices into ones that were functionally connected. In addition, we have discovered that this effect is mainly caused by a gating function played by the subiculum on hippocampal outputs, thus indicating that this limbic structure modulates interactions between hippocampal and parahippocampal networks.

The 4AP model revisited in the light of different patterns of epileptiform activity

We have reported that in reciprocally interconnected hippocampus–EC slices obtained from adult rat (Benini *et al.* 2003) or mouse brains (Barbarosie & Avoli, 1997; Barbarosie *et al.* 2000), application of 4AP-containing or Mg^{2+}-free medium induces CA3-driven interictal events that propagate to the EC where they control the propensity of this latter structure to generate ictal discharges resembling those seen in MTLE patients (cf. Swartzwelder *et al.* 1987; Wilson *et al.* 1988). Accordingly, cutting the Schaffer collaterals in these functionally connected slices averts CA3 outputs and discloses NMDA receptor-mediated ictal events in the EC, thus leading to a pattern of epileptiform activity similar to what is recorded in functionally disconnected slices (Avoli *et al.* 1996; Benini *et al.* 2003).

Until now, we assumed that the inability of CA3-driven interictal activity to propagate to the EC was caused by the slicing procedure that had led to damaging the connections between hippocampus proper and EC. Contrary to this view, we have discovered here that $GABA_A$ receptor antagonism can reversibly transform a disconnected slice into one that appears to be functionally connected. Hence, these findings demonstrate that the two patterns of electrographic activity may not reflect anatomical differences, but rather implicate a mechanism that rests on the gating role played by subicular networks on the propagation of epileptiform discharges originating in the hippocampus proper.

Subicular networks gate hippocampal outputs via $GABA_A$ receptor-mediated mechanisms in functionally disconnected slices

By using sequential recordings along the CA3–CA1–subiculum axis of functionally disconnected slices we have found that the amplitude of the 4AP-induced interictal activity decreases dramatically in the subiculum, where it is often non-existent. Moreover, during $GABA_A$ receptor antagonism, the subiculum undergoes the most dramatic potentiation in field activity (150–550%) signalling an increased recruitment of neurones.

It has been established that disinhibition unmasks polysynaptic excitation within CA3 neuronal networks (Miles & Wong, 1987; Miles *et al.* 1988) and it is possible that this improved synchronicity would consequently lead to an increased drive onto the subiculum. Local pharmacological activation of the subiculum would have been ideal for clarifying this issue. However, initial attempts at focal applications of picrotoxin were elusive due to the fact that in our horizontal slice preparation the subiculum lies critically close to other structures (CA1, dentate gyrus, and medial EC) and dispersion of the droplet to these areas could not be avoided.

Figure 4. NMDA receptors do not contribute to picrotoxin-induced synchronicity in a functionally disconnected slice
A, simultaneous field potential recordings in EC, subiculum (Sub) and CA3 showing that interictal discharges initiating in CA3 do not propagate to the EC where activity is characterized by robust ictal discharges. Note that in this slice no field activity was recorded in the subiculum. *B*, bath application of high concentrations of the NMDA-receptor antagonist CPP results in the loss of EC-driven ictal events. *C*, subsequent application of picrotoxin results in an initial ictal discharge in EC that is followed by a pattern of interictal discharge in all limbic structures. *D*, CPP washout causes a prolongation of the interictal events and a slow down in their frequency of occurrence. These discharges continue to initiate in CA3 and propagate sequentially to the subiculum and EC (inset).

This being said, our observations strongly suggest that although increased presynaptic release of excitatory transmitters at CA1–subiculum synapses may occur, this mechanism is unlikely by itself to explain the amplification of subicular activity observed under $GABA_A$ receptor antagonism. First, potentiation of subicular activity upon $GABA_A$-receptor antagonism was observed even when the subiculum was separated from CA3/CA1 via microknife cuts to the Schaffer collaterals. Furthermore, significant augmentation in activity was demonstrated to occur in isolated subicular minislices in the absence of either upstream or downstream factors. Altogether this is conclusive evidence that the picrotoxin-induced effect in the subiculum is not due to enhanced output of upstream structures (i.e. CA3/CA1) but rather due to the decreased control of GABAergic circuits within the subiculum itself.

Investigation into the functional role of GABAergic circuits within the subiculum was made possible by the interesting property of the 4AP model used in our study. In addition to blocking K^+ currents (Rudy, 1988) and interfering with Ca^{2+} channels (Segal & Barker, 1986), 4AP has been shown to facilitate neurotransmitter release at presynaptic terminals of both excitatory and inhibitory synapses (Thesleff, 1980; Rutecki *et al.* 1987; Aram *et al.* 1991). Previous studies have shown that the subiculum is indeed capable of generating robust interictal discharges under conditions of decreased inhibition (Harris & Stewart,

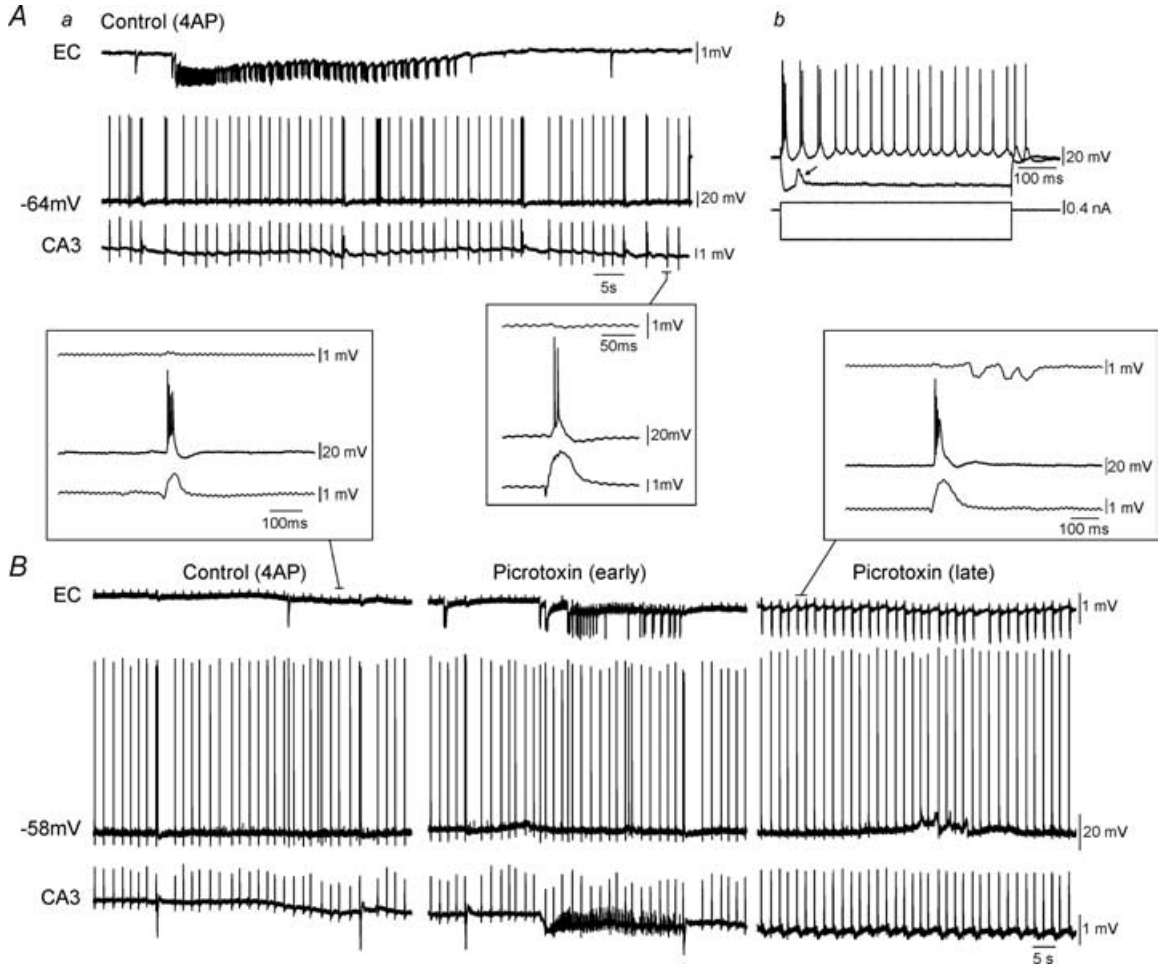

Figure 5. Simultaneous field and intracellular recordings in functionally disconnected slice
Aa, simultaneous field (EC, CA3) and intracellular (subiculum, −64 mV) recordings under control conditions (i.e. 4AP) reveal that this subicular cell is excitable at RMP. Note in the inset that the burst firing generated by this subicular neurone is synchronous with the interictal discharge recorded in CA3, but that no propagation occurs to EC. *Ab*, responses to intracellular injection of depolarizing and hyperpolarizing current pulses; note that this neurone is an intrinsic burster. Depolarizing event during hyperpolarization represents a spontaneously occurring EPSP (arrow). *B*, picrotoxin application to another functionally disconnected slice results in an initial ictal event in EC (Picrotoxin (early)) followed by synchronization of all limbic networks (Picrotoxin (late)). Note in the expanded traces that the intracellularly recorded subicular bursts follow CA3 field activity and precede that of the EC.

2001) or increased excitation (Behr & Heineman, 1996; Harris & Stewart, 2001). Using our model we have, however, shown that the subiculum does not generate robust activity when both excitatory and inhibitory mechanisms are simultaneously altered. Furthermore, we found in the isolated subiculum that under such conditions, this structure is more likely to generate slow synchronous events that are resistant to glutamatergic antagonists but sensitive to $GABA_A$ receptor blockade. These synchronous potentials, which have been reported in other hippocampal structures as well as in the neocortex, represent the activity of highly synchronized interneuronal networks (Perreault & Avoli, 1989, 1992; Michelson & Wong, 1994; Avoli *et al.* 1994, 1996; Lamsa & Kaila, 1997). Altogether, these findings indicate that the overall activity of the subiculum in the presence of 4AP is dominated by inhibitory mechanisms that control hippocampal output propagation to the EC. Blockade of $GABA_A$ receptors hampers this inhibition (as suggested by the decrease in IPSPs recorded in 'silent' subicular cells), allowing an increased recruitment of subicular networks and the consequent spread of both spontaneous and stimulus-induced activity from the hippocampus to the EC.

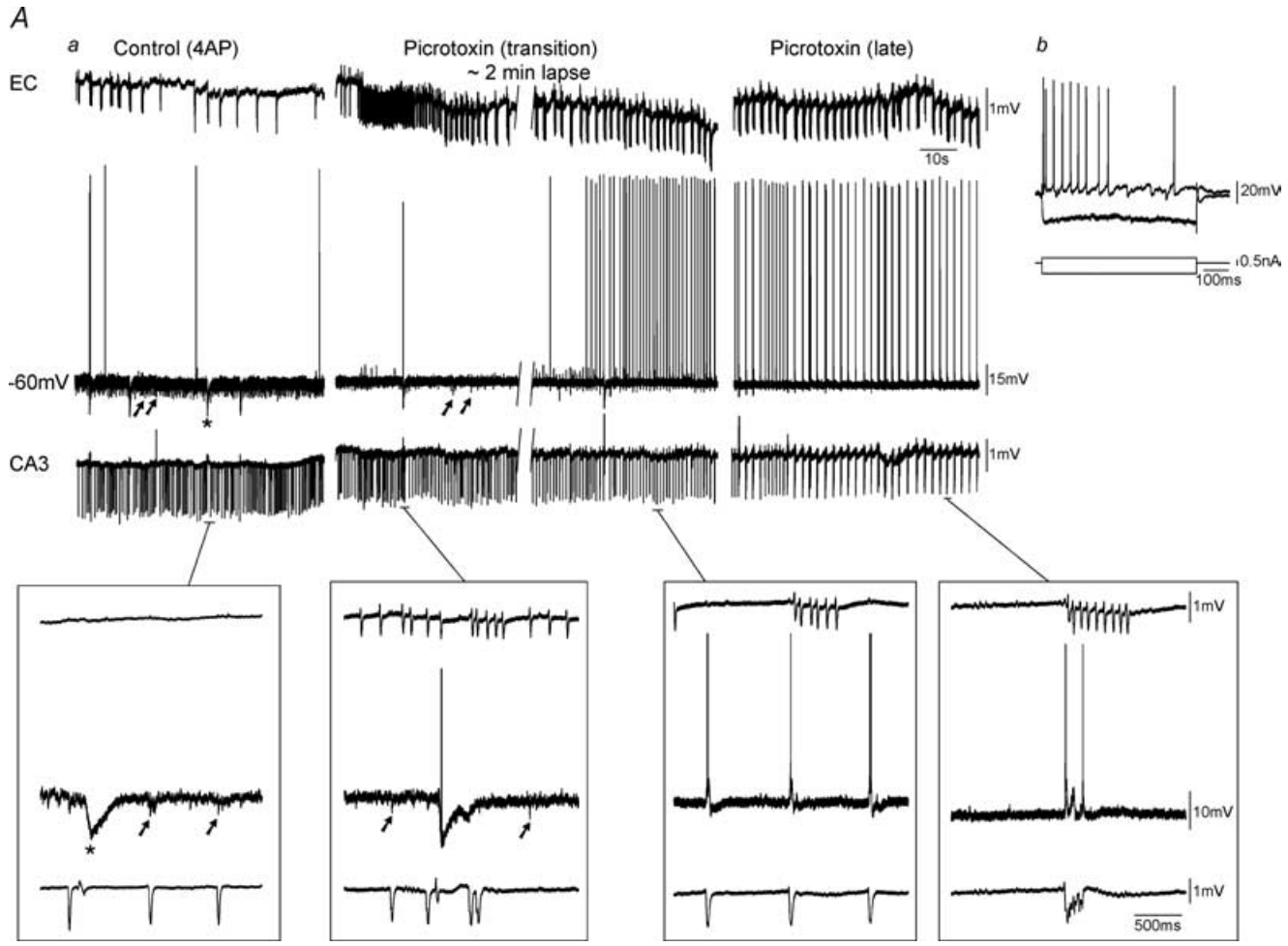

Figure 6. Field and intracellular recordings in functionally disconnected slice
Aa, simulatneous field (EC, CA3) and intracellular (subiculum, −60 mV) recordings during control (4AP) conditions reveals that this subicular cell is 'silent' at RMP. Note the presence of PSPs that are coincident with CA3 discharges (arrows) and the large isolated inhibitory postsynaptic potentials (IPSPs) (Control (4AP), asterisk). Superfusion of slices with picrotoxin discloses in these cells action potential discharges at RMP (Picrotoxin). Monitoring the evolution in the intracellular activity of these subicular neurones from the initial application of the $GABA_A$ receptor antagonist (Picrotoxin (transition)) until the complete synchronization between hippocampal and parahippocampal structures (Picrotoxin (late)) reveals IPSP disappearance. Insets below traces demonstrate expansions of selected events. Note the presence of large IPSPs (asterisk) and smaller PSPs (arrows) within the subiculum prior to complete synchronization of limbic structures. *Ab*, firing properties of this cell reveal a non-bursting neurone.

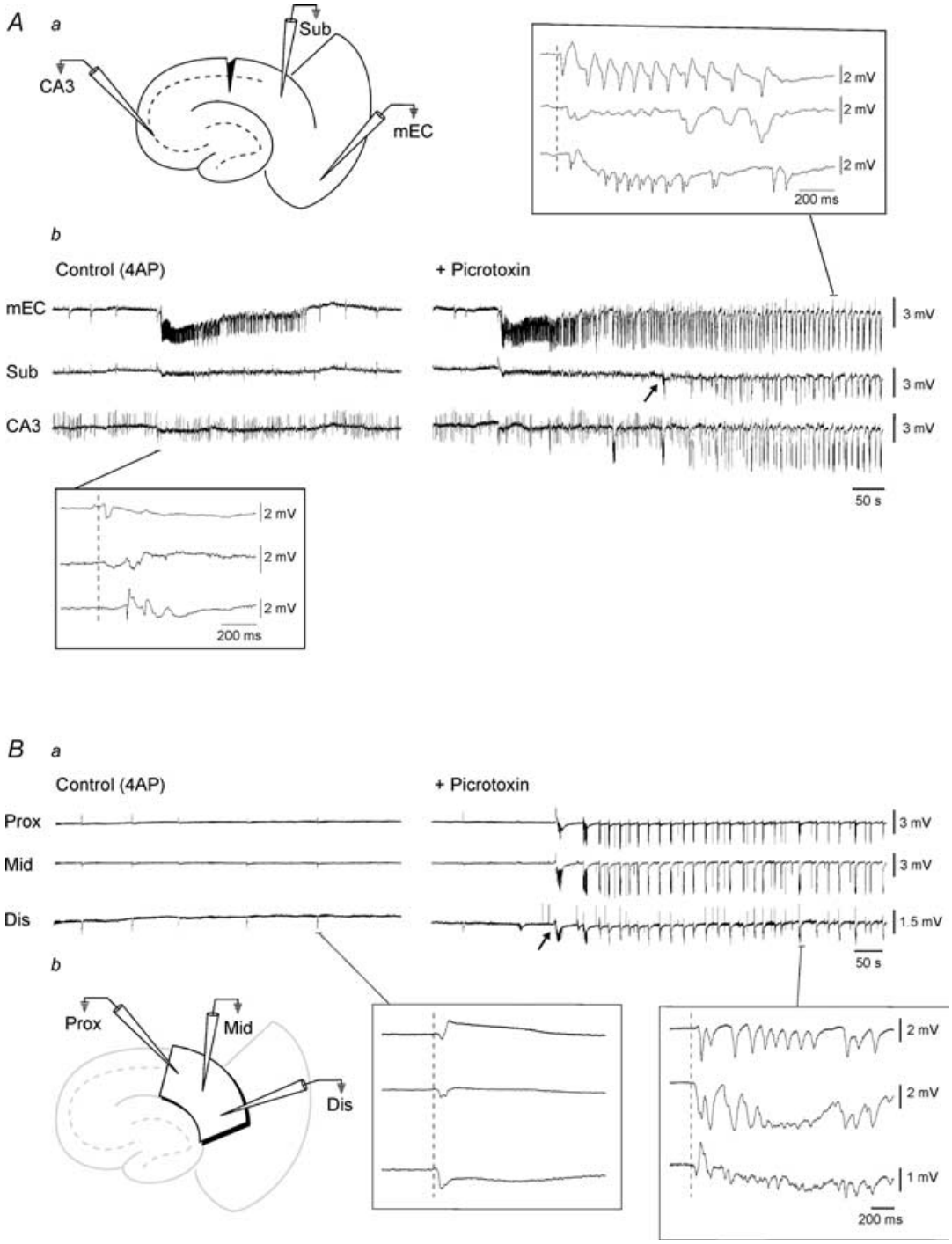

Figure 7. Picrotoxin-induced potentiation of subicular activity is not due to upstream effects
Aa, diagram illustrating a combined slice in which the Schaffer collaterals have been severed by a microknife cut at the level of CA1. *Ab*, simultaneous field potential recordings obtained from this slice preparation in EC, subiculum (Sub) and CA3 during bath application of 4AP and upon further addition of Picrotoxin. The slow interictal events observed in all structures in the presence of 4AP initiate in EC (bottom inset). Note the potentiation of subicular activity that occurs in the presence of the $GABA_A$ receptor antagonist (arrow). Also note that in the presence of picrotoxin, the epileptiform activity in this case initiates in EC and subsequently spreads to subiculum and CA3 (upper inset). *Ba*, simultaneous field potential recordings obtained from the proximal, middle and distal regions of an isolated subicular minislice preparation during 4AP application and upon further addition of Picrotoxin. Note that during 4AP, slow interictal-like events are generated in all regions of the subiculum (left inset). Also note that $GABA_A$ receptor antagonism induces potentiation of subicular activity in all regions (arrow indicates onset of picrotoxin-induced activity). Right inset illustrates expansion of picrotoxin-induced event. *Bb*, diagram illustrating the isolated minislice preparation and position of field electrodes.

Subicular cells may be under a different degree of $GABA_A$ receptor-mediated control in the same functionally disconnected slice

Neurophysiological investigations have shown that several types of GABAergic cells are present in the subiculum (Kawaguchi & Hama, 1987; Greene & Totterdell, 1997; Menendez de la Prida *et al.* 2003). We have found here that under control conditions (i.e. during application of medium containing 4AP only) subicular pyramidal neurones generate two different patterns of intracellular activity in functionally disconnected slices: one group of cells fired action potentials in coincidence with CA3-driven interictal events whilst the other generated either EPSP–IPSP sequences or isolated IPSPs. These two behaviours of subicular cells, both of which could be found in the same slice, have also been reported in the human epileptic subiculum of MTLE patients, where they reflect differences in the reversal potential of pyramidal cells for $GABA_A$ receptor-mediated conductances (Cohen *et al.* 2002).

The presence of 'silent' subicular cells in functionally disconnected slices indicates that hippocampal activity may not propagate to the EC due to local inhibitory

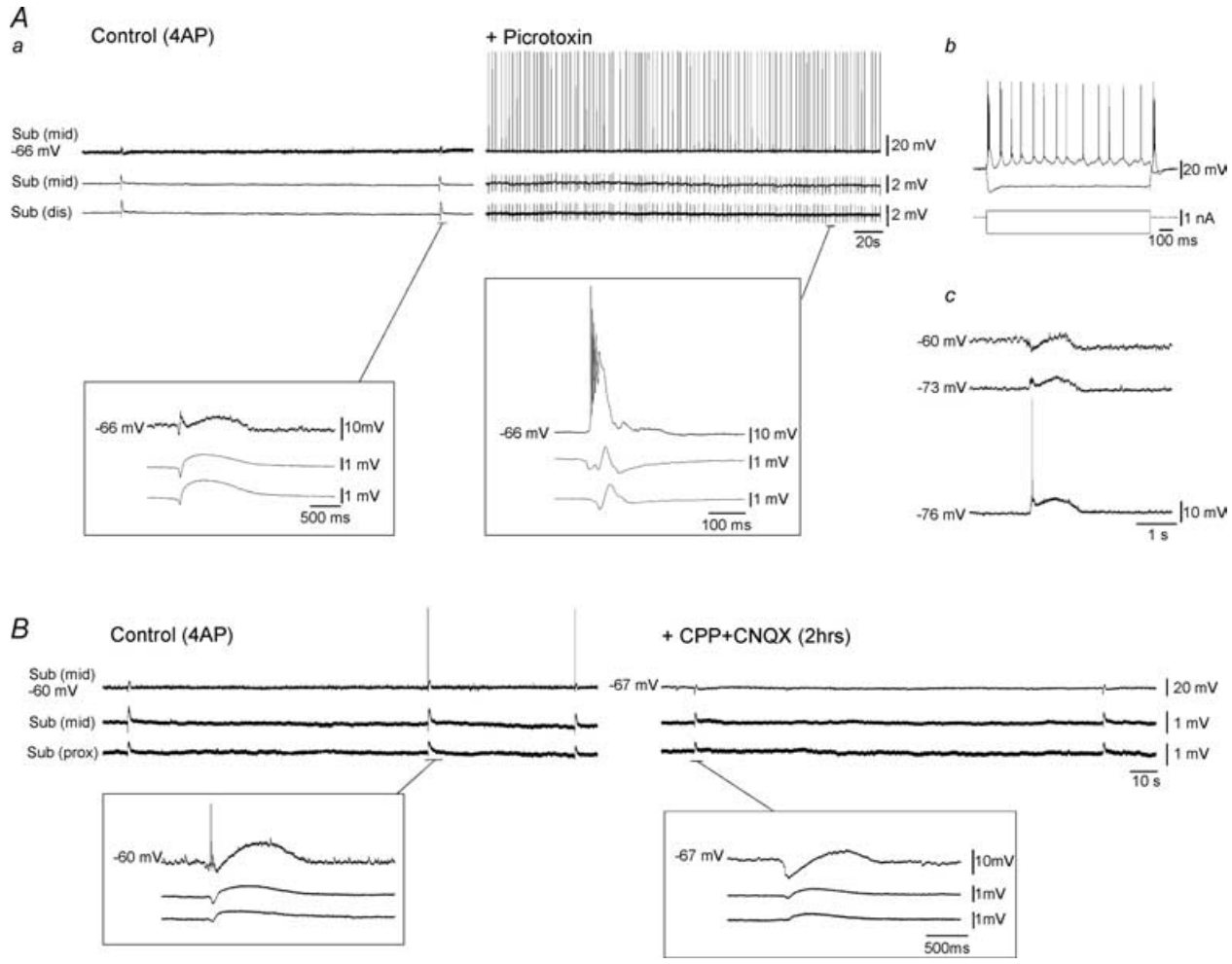

Figure 8. Pharmacological characterization of 4AP-induced activity in isolated subicular minislices
Aa, simulatneous field (middle subiculum, distal subiculum) and intracellular (middle subiculum, −66 mV) recordings during control (4AP) conditions reveals that the slow interictal events correspond intracellularly to an early hyperpolarization followed by a sustained depolarization (left inset). In the presence of picrotoxin there is increased field activity in the isolated subiculum and robust network bursting can be recorded intracellularly (right inset). *Ab*, firing properties of this cell reveals that it was an intrinsically bursting neurone. *Ac*, intracellular traces of the 4AP-induced event at different membrane potentials reveals reversal of the hyperpolarizing component at negative membrane potentials (−73 mV and −76 mV). Note the truncated action potential riding on this reversed event at −76 mV. *Ba*, simulatneous field (middle subiculum, proximal subiculum) and intracellular (middle subiculum, −60 mV and −67 mV) recordings in control (4AP) and after 2 h of further CPP + CNQX application. Note that intracellular recordings were carried out from two different cells within the same slice and in the same subicular region. Insets demonstrate expansions of the slow synchronouns event during both conditions.

control exerted on a subset of projecting subicular cells. In line with this view, previous studies have demonstrated that subicular pyramidal cells are restrained by local GABAergic networks via feedforward (Finch & Babb, 1980; Colino & De Molina, 1986; Finch *et al.* 1988; Behr *et al.* 1998) and recurrent inhibitory mechanisms (Menendez de la Prida, 2003; Menendez de la Prida & Gal, 2004). Accordingly, we have demonstrated that IPSP blockade by $GABA_A$ receptor antagonism coincides with the appearance of network-driven burst firing, thus implicating a role for subicular $GABA_A$ receptor-mediated inhibition in gating hippocampal output activity. Indeed, it has been reported that epileptiform discharges generated in the hippocampus can successfully propagate to the medial EC via the subicular complex under reduction of GABAergic mechanisms (Menendez de la Prida & Pozo, 2002).

Conclusions

Studies in various epilepsy models have identified the dentate gyrus as a gater for the spread of limbic seizures from the EC to the hippocampus proper (Collins *et al.* 1983; Heinemann *et al.* 1992). However, until this study, no investigation had addressed the role of the subiculum in controlling hippocampal outputs during epileptiform synchronization even though it was well established that this structure is in a strategic position for doing so. Our observations that blocking $GABA_A$ receptor-mediated mechanisms results in subicular hyperexcitability and subsequently intralimbic synchronization is relevant to pathological conditions such as epilepsy. Studies in slices obtained from MTLE patients indicate that both bursting pyramidal cells and interneurones contribute to the interictal activity that occurs in the subiculum (Cohen *et al.* 2002; Wozny *et al.* 2003). In addition, in chronic animal models of MTLE, alterations at the level of intrinsic and network properties of principal cells (Wellmer *et al.* 2002; Knopp *et al.* 2005) as well as a reduction in specific interneuronal subpopulations (van Vliet *et al.* 2004) have been reported in this structure. Altogether, these findings suggest that synaptic reorganization and altered inhibition contribute to subicular network hyperexcitability that may in turn play a role in the generation and spread of convulsive activity.

References

Aram JA, Michelson HB & Wong RK (1991). Synchronized GABAergic IPSPs recorded in the neocortex after blockade of synaptic transmission mediated by excitatory amino acids. *J Neurophysiol* **65**, 1034–1041.

Avoli M, Barbarosie M, Lücke A, Nagao T, Lopantsev V & Köhling R (1996). Synchronous GABA-mediated potentials and epileptiform discharges in the rat limbic system in vitro. *J Neurosci* **16**, 3912–3924.

Avoli M, Mattia D, Siniscalchi A, Perreault P & Tomaiuolo F (1994). Pharmacology and electrophysiology of a synchronous GABA-mediated potential in the human neocortex. *Neuroscience* **62**, 655–666.

Barbarosie M & Avoli M (1997). CA3-driven hippocampal-entorhinal loop controls rather than sustains in vitro limbic seizures. *J Neurosci* **17**, 9308–9314.

Barbarosie M, Louvel J, Kurcewicz I & Avoli M (2000). CA3-released entorhinal seizures disclose dentate gyrus epileptogenicity and unmask a temporoammonic pathway. *J Neurophysiol* **83**, 1115–1124.

Behr J, Gloveli T & Heinemann U (1998). The perforant path projection from the medial entorhinal cortex layer III to the subiculum in the rat combined hippocampal-entorhinal cortex slice. *Eur J Neurosci* **10**, 1011–1018.

Behr J & Heinemann U (1996). Low Mg^{2+} induced epileptiform activity in the subiculum before and after disconnection from rat hippocampal and entorhinal cortex slices. *Neurosci Lett* **205**, 25–28.

Benini R, D'Antuono M, Pralong E & Avoli M (2003). Involvement of amygdala networks in epileptiform synchronization in vitro. *Neuroscience* **120**, 75–84.

Canteras NS & Swanson LW (1992). Projections of the ventral subiculum to the amygdala, septum, and hypothalamus: a PHAL anterograde tract-tracing study in the rat. *J Comp Neurol* **324**, 180–194.

Cohen I, Navarro V, Clemenceau S, Baulac M & Miles R (2002). On the origin of interictal activity in human temporal lobe epilepsy in vitro. *Science* **298**, 1418–1421.

Colino A & Fernandez de Molina A (1986). Inhibitory response in entorhinal and subicular cortices after electrical stimulation of the lateral and basolateral amygdala of the rat. *Brain Res* **378**, 416–419.

Collins RC, Tearse RG & Lothman EW (1983). Functional anatomy of limbic seizures: Focal discharges from medial entorhinal cortex in rat. *Brain Res* **280**, 25–40.

D'Antuono M, Benini R, Biagini G, D'Arcangelo G, Barbarosie M, Tancredi V *et al.* (2002). Limbic network interactions leading to hyperexcitability in a model of temporal lobe epilepsy. *J Neurophysiol* **87**, 634–639.

Deacon TW, Eichenbaum H, Rosenberg P & Eckmann KW (1983). Afferent connections of the perirhinal cortex in the rat. *J Comp Neurol* **220**, 168–190.

Du F, Whetsell WO Jr, Abou-Khalil B, Blumenkopf B, Lothman EW & Schwarcz R (1993). Preferential neuronal loss in layer III of the entorhinal cortex in patients with temporal lobe epilepsy. *Epilepsy Res* **16**, 223–233.

Finch DM & Babb TL (1980). Inhibition in subicular and entorhinal principal neurons in response to electrical stimulation of the fornix and hippocampus. *Brain Res* **196**, 89–98.

Finch DM & Babb TL (1981). Demonstration of caudally directed hippocampal efferents in the rat by intracellular injection of horseradish peroxidase. *Brain Res* **214**, 405–410.

Finch DM, Tan AM & Isokawa-Akesson M (1988). Feedforward inhibition of the rat entorhinal cortex and subicular complex. *J Neurosci* **8**, 2213–2226.

Gloor P (1997). *The Temporal Lobe and Limbic System.* Oxford University Press, New York.

Greene JR & Totterdell S (1997). Morphology and distribution of electrophysiologically defined classes of pyramidal and nonpyramidal neurons in rat ventral subiculum in vitro. *J Comp Neurol* **380**, 395–408.

de Guzman P, D'Antuono M & Avoli M (2004). Initiation of electrographic seizures by neuronal networks in entorhinal and perirhinal cortices in vitro. *Neurosci* **123**, 875–886.

Harris E & Stewart M (2001). Intrinsic connectivity of the rat subiculum. II. Properties of synchronous spontaneous activity and a demonstration of multiple generator regions. *J Comp Neurol* **435**, 506–518.

Heinemann U, Beck H, Dreier JP, Ficker E, Stabel J & Zhang CL (1992). The dentate gyrus as a regulated gate for the propagation of epileptiform activity. *Epilepsy Res Suppl* **7**, 273–280.

Houser CR (1999). Neuronal loss and synaptic reorganization in temporal lobe epilepsy. *Adv Neurol* **79**, 743–761.

Houser CR, Miyashiro JE, Swartz BE, Walsh GO, Rich JR & Delgado-Escueta AV (1990). Altered patterns of dynorphin immunoreactivity suggest mossy fiber reorganization in human hippocampal epilepsy. *J Neurosci* **10**, 267–282.

Kawaguchi Y & Hama K (1987). Fast-spiking non-pyramidal cells in the hippocampal CA3 region, dentate gyrus and subiculum of rats. *Brain Res* **425**, 351–355.

Knopp A, Kivi A, Wozny C, Heinemann U & Behr J (2005). Cellular and network properties of the subiculum in the pilocarpine model of temporal lobe epilepsy. *J Comp Neurol* **483**, 476–488.

Lamsa K & Kaila K (1997). Ionic mechanisms of spontaneous GABAergic events in rat hippocampal slices exposed to 4-aminopyridine. *J Neurophysiol* **78**, 2582–2591.

Menendez de la Prida L (2003). Control of bursting by local inhibition in the rat subiculum in vitro. *J Physiol* **549**, 219–230.

Menendez de la Prida L & Gal B (2004). Synaptic contributions to focal and widespread spatiotemporal dynamics in the isolated rat subiculum in vitro. *J Neurosci* **24**, 5525–5536.

Menendez de la Prida L & Pozo MA (2002). Excitatory and inhibitory control of epileptiform discharges in combined hippocampal/entorhinal cortical slices. *Brain Res* **940**, 27–35.

Menendez de la Prida L, Suarez F & Pozo MA (2003). Electrophysiological and morphological diversity of neurons from the rat subicular complex in vitro. *Hippocampus* **13**, 728–744.

Michelson HB & Wong RK (1994). Synchronization of inhibitory neurones in the guinea-pig hippocampus in vitro. *J Physiol* **477**, 35–45.

Miles R, Traub RD & Wong RK (1988). Spread of synchronous firing in longitudinal slices from the CA3 region of the hippocampus. *J Neurophysiol* **60**, 1481–1496.

Miles R & Wong RK (1987). Inhibitory control of local excitatory circuits in the guinea-pig hippocampus. *J Physiol* **388**, 611–629.

O'Mara SM, Commins S, Anderson M & Gigg J (2001). The subiculum: a review of form, physiology and function. *Prog Neurobiol* **64**, 129–155.

Perreault P & Avoli M (1989). Effects of low concentrations of 4-aminopyridine on CA1 pyramidal cells of the hippocampus. *J Neurophysiol* **61**, 953–970.

Perreault P & Avoli M (1992). 4-Aminopyridine-induced epileptiform activity and a GABA-mediated long-lasting depolarization in the rat hippocampus. *J Neurosci* **12**, 104–115.

Pitkanen A, Tuunanen J, Kalviainen R, Partanen K & Salmenpera T (1998). Amygdala damage in experimental and human temporal lobe epilepsy. *Epilepsy Res* **32**, 233–253.

Rudy B (1988). Diversity and ubiquity of K channels. *Neuroscience* **25**, 729–749.

Rutecki PA, Lebeda FJ & Johnston D (1987). 4-Aminopyridine produces epileptiform activity in hippocampus and enhances synaptic excitation and inhibition. *J Neurophysiol* **57**, 1911–1924.

Segal M & Barker JL (1986). Rat hippocampal neurons in culture: Ca^{2+} and Ca^{2+}-dependent K^{+} conductances. *J Neurophysiol* **55**, 751–766.

Staff NP, Jung HY, Thiagarajan T, Yao M & Spruston N (2000). Resting and active properties of pyramidal neurons in subiculum and CA1 of rat hippocampus. *J Neurophysiol* **84**, 2398–2408.

Sutula T, Cascino G, Cavazos J, Parada I & Ramirez L (1989). Mossy fiber synaptic reorganization in the epileptic human temporal lobe. *Ann Neurol* **26**, 321–330.

Swanson LW & Cowan WM (1977). An autoradiographic study of the organization of the efferent connections of the hippocampal formation in the rat. *J Comp Neurol* **172**, 49–84.

Swanson LW, Wyss JM & Cowan WM (1978). An autoradiographic study of the organization of intrahippocampal association pathways in the rat. *J Comp Neurol* **181**, 681–715.

Swartzwelder SH, Lewis DV, Anderson WW & Wilson WA (1987). Seizure-like events in brain slices: supression by interictal activity. *Brain Res* **410**, 362–366.

Thesleff S (1980). Aminopyridines and synaptic transmission. *Neuroscience* **5**, 1413–1419.

Traub RD, Borck C, Colling SB & Jefferys JGR (1996). On the structure of ictal events in vitro. *Epilepsia* **37**, 879–891.

van Vliet EA, Aronica E, Tolner EA, Lopes da Silva FH & Gorter JA (2004). Progression of temporal lobe epilepsy in the rat is associated with immunocytochemical changes in inhibitory interneurons in specific regions of the hippocampal formation. *Exp Neurol* **187**, 367–379.

Wellmer J, Su H, Beck H & Yaari Y (2002). Long-lasting modification of intrinsic discharge properties in subicular neurons following status epilepticus. *Eur J Neurosci* **16**, 259–266.

Wiebe S (2000). Epidemiology of temporal lobe epilepsy. *Can J Neurol Sci* **27** (Suppl. 1), S6–S10.

Wilson WA, Swartzwelder HS, Anderson WW & Lewis DV (1988). Seizure activity in vitro: a dual focus model. *Epilepsy Res* **2**, 289–293.

Witter MP, Groenewegen HJ, Lopes da Silva FH & Lohman AH (1989). Functional organization of the extrinsic and intrinsic circuitry of the parahippocampal region. *Prog Neurobiol* **33**, 161–253.

Witter MP, Ostendorf RH & Groenewegen HJ (1990). Heterogeneity in the dorsal subiculum of the rat. distinct neuronal zones project to different cortical and subcortical targets. *Eur J Neurosci* **2**, 718–725.

Wozny C, Kivi A, Lehmann TN, Dehnicke C, Heinemann U & Behr J (2003). Comment on 'On the origin of interictal activity in human temporal lobe epilepsy in vitro'. *Science* **301**, 463.

Yilmazer-Hanke DM, Wolf HK, Schramm J, Elger CE, Wiestler OD & Blumcke I (2000). Subregional pathology of the amygdala complex and entorhinal region in surgical specimens from patients with pharmacoresistant temporal lobe epilepsy. *J Neuropathol Exp Neurol* **59**, 907–920.

Acknowledgements

This study was supported by the Canadian Institutes of Health Research (Grant MOP-8109). We thank Ms T. Papadopoulos for secretarial assistance.